



EXPERIMENTAL INVESTIGATION OF ECCENTRIC REINFORCED CONCRETE BEAM-COLUMN-SLAB CONNECTIONS UNDER EARTHQUAKE LOADING

BURCU BURAK¹ AND JAMES K. WIGHT²

SUMMARY

The inelastic behavior of beam-to-column joints has been studied since 1960's; however, there is still limited information on eccentric connections, in which the centerline of the spandrel beam does not coincide with the centroid of the column. In this experimental study, the seismic behavior of three 3/4-scale eccentric beam-column-slab subassemblies was investigated. The main design parameters were selected as the eccentricity, normal beam width, and column section aspect ratio. The eccentricity between the centerline of the spandrel beam and centroidal axis of the column was selected as a design variable because some buildings with eccentric spandrel beams exhibited extensive damage during earthquakes and previous tests of planar (two-dimensional) specimens indicated early deterioration of joint shear strength for these types of structures. The main design variable for the column was the section aspect ratio (width vs. depth) to examine if the entire joint region of the rectangular column works under applied shear loading as effectively as a square column. Each specimen was tested twice. First, lateral loading was applied in the plane of the spandrel beam, then the specimen was rotated 90 degrees and the loading was applied in the plane of the normal beam that is perpendicular to the spandrel beam. The major design variable for the normal beam was its width, which was larger than the width of the supporting column for the last test specimen, to investigate the confinement of the joint region provided by the wide normal beams, and the transfer of moment from the wide beam to the column by a previously loaded spandrel beam. The experimental results indicated that when exterior connections have the floor system with slab and beams spanning in two perpendicular directions, the influence of the spandrel beam eccentricity on the seismic behavior of the joint region changes significantly. When the specimens were compared to previous tests, it was observed that the damage in the joint region was not as severe, the specimens have full hysteresis curves with high energy dissipation capacities, and the deterioration of joint shear stiffness and strength were delayed due to the additional torsional stiffness resulting from the use of a floor system.

¹ Ph.D. Candidate, Department of Civil and Environmental Engineering, University of Michigan, Ann Arbor, USA, Email: bburak@engin.umich.edu

² Professor, Department of Civil and Environmental Engineering, University of Michigan, Ann Arbor, USA, Email: jwight@engin.umich.edu

INTRODUCTION

Eccentric connections, in which the axis of the spandrel beam is offset from the axis of the column, are used in exterior frames of reinforced concrete buildings due to architectural considerations. In this type of connection, the spandrel beams, which are narrower than the column, are generally flush with the exterior face of the column. The eccentricity between the beam and the column results in the development of torsion in the connection region under lateral loading parallel to the exterior edge of the subassembly. This torsion in the joint produces additional shear stresses and affects the shear capacity of the joint.

An experimental investigation was carried out to develop new data and to further study the cyclic behavior of eccentric connections. Three 3/4-scale exterior reinforced concrete beam-column-slab connections were tested under reversed cyclic loading. The specimens are three-dimensional and consist of two spandrel beams, a normal beam in the transverse direction, and a floor slab. Lateral load was applied in two principal directions, one plane at a time, to determine the effect of prior loading on performance of the connection. First, a control specimen, designed following the recommendations of ACI-ASCE Committee 352 [1] and ACI 318-99 [2], was tested. Based on the test results, the other specimens were designed by modifying the eccentricity, beam and column section aspect ratios, and the level of joint shear stress to examine their effect on joint behavior. The performance of the eccentric connections was evaluated by examining the cracking pattern, lateral load versus story drift response, beam rotations, energy dissipation capacity, and stiffness deterioration of the specimens.

One of the main design variables was selected to be the eccentricity of the spandrel beam with respect to the column. Prior tests [3, 4], without a normal beam and a floor slab, have indicated that the eccentricity of the spandrel beam leads to unsymmetrical damage in the joint, early deterioration of the joint shear strength, and loss of anchorage for the spandrel beam reinforcement. In addition, some buildings with eccentric spandrel beams exhibited extensive damage under earthquake loading, while other reinforced concrete buildings in the same area showed very little or no damage [5, 6].

The major design variable for the column is taken as the section aspect ratio (width vs. depth). The experimental program by Raffaele and Wight [3] indicated that the effective joint width for resisting shear force depends on the column section aspect ratio. Therefore, both square and rectangular columns were tested in this experimental program to study the correlation between the column section aspect ratio and the effective joint width.

The width of the normal beam was chosen as another design variable. The last specimen was built as a wide-beam structure in which the normal beam width was larger than the column width. In a wide-beam structure, some of the beam longitudinal reinforcement is anchored in the spandrel beams outside the column core. Wide beam longitudinal reinforcement anchored in the column core transfers tension directly to the column. The remaining reinforcement anchored in the spandrel beams transfers tension to the column through torsion in the spandrel beam. If the spandrel beam is unable to transmit the applied torsion from the wide beam to the column, the full moment strength of the wide beam cannot be developed. The last specimen provides information on the effect of prior loading on the bond strength of the wide beam reinforcement anchored in the spandrel beam.

EXPERIMENTAL PROGRAM

Test Setup and Specimens

Three exterior reinforced concrete beam-column-slab subassemblies were tested under reversed cyclic loading. Each specimen consists of top and bottom columns, two spandrel beams, a normal beam, and a floor slab. The spandrel beams are flush with the exterior face of the column, which results in an eccentricity between the centerline of the beam and the centroidal axis of the column. The normal beam in the transverse direction makes a concentric connection with the column. Columns and beams are pin supported at their mid-heights and mid-spans, where inflection points are likely to occur during a seismic event. The specimens were subjected to quasi-static cyclic loading in two principal directions, one plane at a time. They were loaded initially in the spandrel beam direction (Fig. 1a), then they were rotated 90 degrees and loaded in the normal beam direction (Fig. 1b). Loading in the spandrel beam direction gives a direct correlation between these three-dimensional specimens and the prior testing of planar specimens with no slab and normal beam. Loading in the normal beam direction enables the determination of the effect of prior loading on performance of the connection.

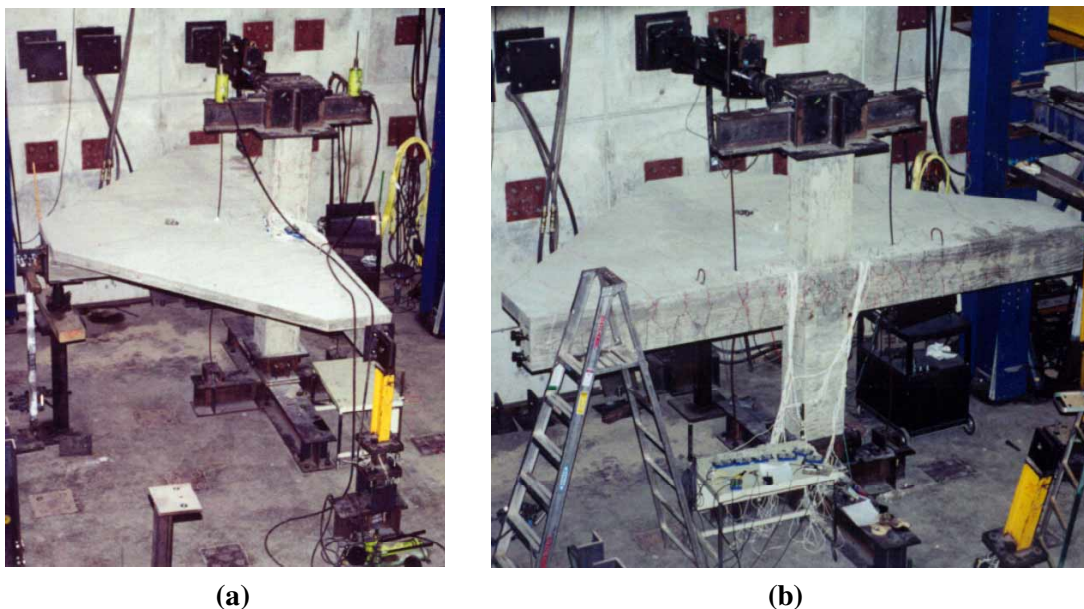


Figure 1: Loading of Specimens in (a) Spandrel and (b) Normal Beam Directions

Fig. 2 shows a sketch of the test setup. An axial load of approximately five percent of the axial capacity of the column was applied with hydraulic jacks. The lateral load was applied horizontally through the top of the column following a predefined displacement history. In each direction, twenty cycles of lateral displacement was applied to each specimen, ranging from 0.5% to 5.0% story drifts to simulate the inelastic loading during an earthquake. Each cycle to a new drift level is applied twice to evaluate the loss of strength and stiffness of the specimens during the repeated cycles. Some 1.0% drift cycles were interspersed into the displacement history to evaluate the residual stiffness of the specimens.

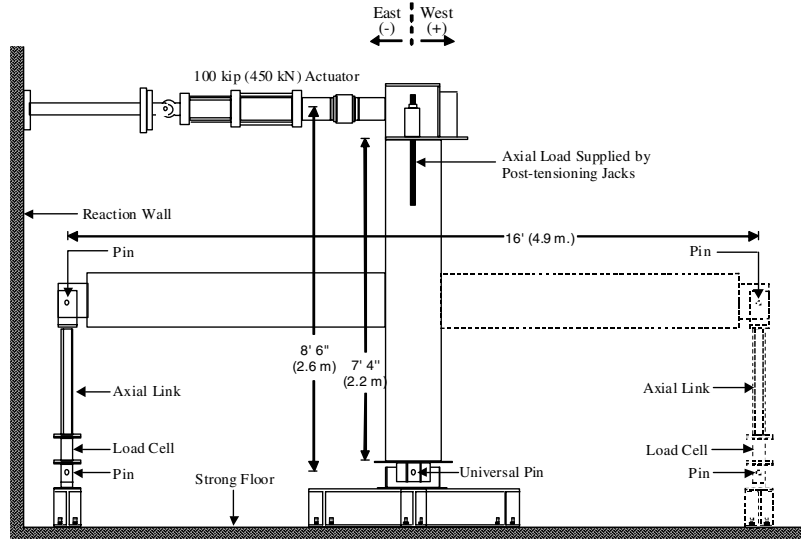


Figure 2: Test Setup

For loading in the spandrel beam direction, the following equation for the effective joint width, b_j , proposed by the second author to ACI-ASCE Committee 352, governed in the design of the specimens:

$$b_j = b_b + \Sigma m h_c/2$$

where,

b_b = design width of beam,

m = slope to define the effective width of joint transverse to the direction of shear. For all the specimens, the eccentricity between the beam centerline and column centroid exceeds $b_b/8$; therefore, $m = 0.3$,

b_c = width of column transverse to the direction of shear,

h_c = depth of column in the direction of load being considered.

For loading in the normal beam direction, the above equation was also checked for the design of the connections using $m = 0.5$, because there is no eccentricity between the normal beam and the column. However, the governing equation turned out to be $(b_b + b_c)/2$. In the third specimen, which has a wide normal beam, the effective joint width was taken as $b_c + (b_b - b_c)/4$, because the equation proposed in the current codes is found to be conservative for wide-beam structures.

Design variables and the dimensions of the specimens are given in Table 1. In order to enforce beam plastic hinging rather than joint failure or column plastic hinging, the strong column-weak beam philosophy ($M_r > 1.0$) was used in the design. Minimum shrinkage and temperature reinforcement was used in both directions of the slab. Specimen 1 is designed as a control specimen following the recommendations of ACI-ASCE Committee 352 [1] and ACI 318-99 [2]. It has a square column and spandrel and normal beams with typical dimensions. Other specimens were designed after the first one was tested; the eccentricity, beam and column section aspect ratios, and the level of joint shear stress were modified to examine their effect on connection performance. For the last two specimens, the spandrel beam eccentricity is almost doubled. Moreover, rectangular columns with a section aspect ratio of 1.5 were used in these specimens to examine the influence of this ratio on the effective joint width. The dimensions of the spandrel and normal beams were also modified to investigate the effect of beam section aspect ratio.

Table 1: Member Dimensions and Design Variables

		Specimen 1	Specimen 2	Specimen 3
Column	Dimensions	14"x14" (356 x 356 mm)	14"x21" (356 x 533 mm)	14"x21" (356 x 533 mm)
	ρ	0.018	0.012	0.012
Spandrel Beam	Dimensions	8"x15" (203 x 381 mm)	10"x18" (254 x 457 mm)	10"x18" (254 x 457 mm)
	ρ_{top}	0.0117	0.0106	0.0106
	ρ_{bottom}	0.0076	0.0057	0.0057
	M_r	1.5	1.1	1.1
	e	3" (76 mm)	5.5" (140 mm)	5.5" (140 mm)
	$h_{col}/d_{b,beam}$	22.4	22.4	22.4
	$h_{beam}/d_{b,col}$	20	24	24
Normal Beam	Dimensions	12"x15" (305 x 381 mm)	12"x18" (305 x 457 mm)	30"x12" (762 x 305 mm)
	ρ_{top}	0.0108	0.0133	0.0157
	ρ_{bottom}	0.0076	0.0097	0.0109
	M_r	1.8	1.7	1.5
	$h_{beam}/d_{b,col}$	20	24	16
Joint	v_{j-S}	$14.1\sqrt{f'_c}$ psi ($1.2\sqrt{f'_c}$ MPa)	$14.4\sqrt{f'_c}$ psi ($1.2\sqrt{f'_c}$ MPa)	$14.4\sqrt{f'_c}$ psi ($1.2\sqrt{f'_c}$ MPa)
	v_{j-N}	$9.4\sqrt{f'_c}$ psi ($0.78\sqrt{f'_c}$ MPa)	$9.1\sqrt{f'_c}$ psi ($0.76\sqrt{f'_c}$ MPa)	$13.1\sqrt{f'_c}$ psi ($1.09\sqrt{f'_c}$ MPa)

ρ = Reinforcement ratio,

M_r = Moment strength ratio; slab included as compression flange for positive bending and slab bars included as tensile reinforcement for negative bending,

e = Eccentricity between the spandrel beam centerline and the centroidal axis of the column,

$h_{col}/d_{b,beam}$ = Ratio of column height to beam bar diameter,

$h_{beam}/d_{b,col}$ = Ratio of beam height to column bar diameter,

v_{j-S} = Design joint shear stress for loading in the spandrel beam direction,

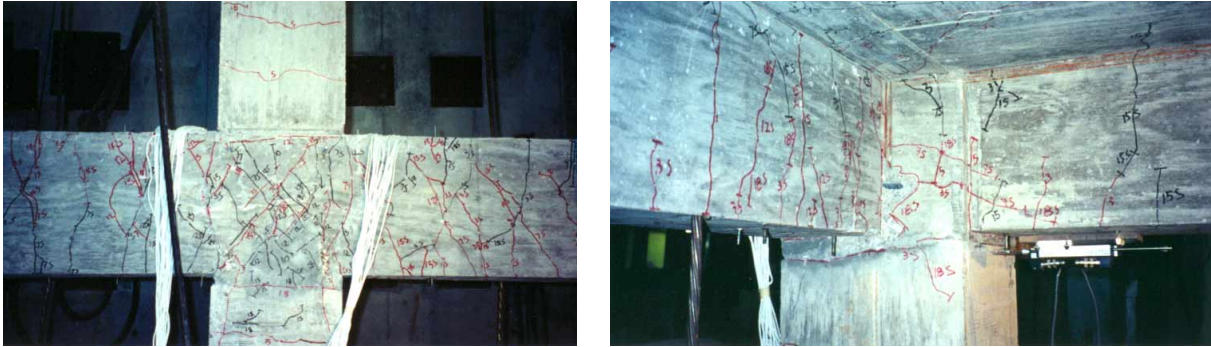
v_{j-N} = Design joint shear stress for loading in the normal beam direction.

EXPERIMENTAL RESULTS

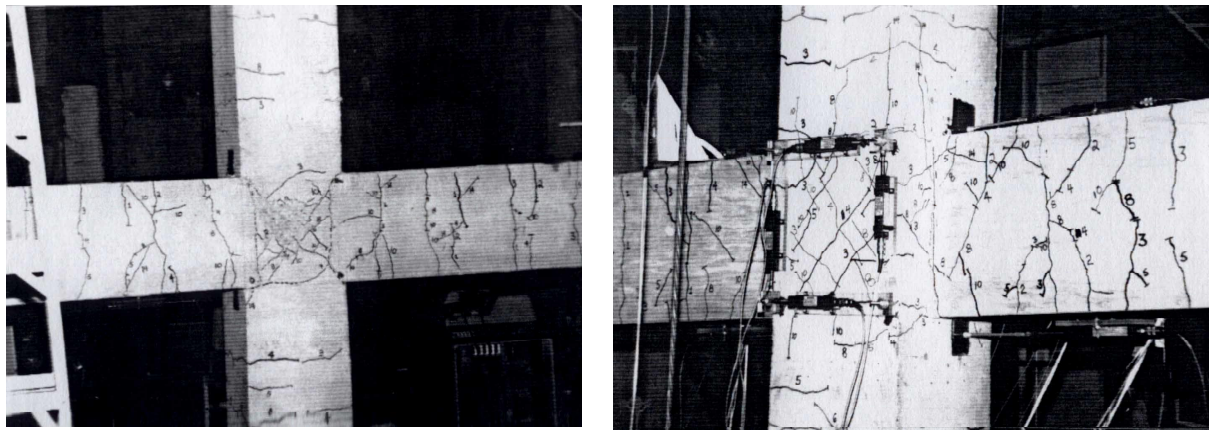
Crack Development

The observed cracking pattern at the exterior and interior faces of Specimen 1 at the end of testing in both directions is given in Fig. 3. During the first test, while loading in the spandrel beam direction, flexural cracks were observed in the spandrel beams at the first cycle to 0.5% drift. Diagonal cracks occurred in the joint region at approximately 1% story drift; however, they remained narrow until the end of the test. The number and width of torsional crack formed in the spandrel beam and connection region were also less than expected. This minor damage correlates well with the maximum measured joint shear deformation of 1.0%. Prior tests [3, 4] indicated that the eccentricity of the spandrel beam leads to

unsymmetrical damage in the joint with severe cracking on the exterior face (Fig. 4). However, Specimen 1 showed only minor damage on both joint faces. For loading in the normal beam direction, flexural cracking of the normal beam started at 0.5% drift for this specimen. Additional diagonal shear cracks formed in the joint after 1% story drift. Even at high drift levels, the specimen exhibited good behavior with almost no spalling of concrete in or near the joint region.



(a) (b)
Figure 3: Cracking Pattern at the (a) Exterior and (b) Interior Faces of Specimen 1



(a) (b)
Figure 4: Cracking Pattern at (a) Exterior and (b) Interior Faces of a Prior Test Specimen [3]

In Specimen 2, the number of cracks increased, the cracks were wider, and spalling of the cover concrete was observed at the exterior face (Fig. 5). For loading in the spandrel beam direction, some torsional cracks were detected in the spandrel beam and the joint region. In this specimen, flexural cracks opened at the face of the joint core region rather than the beam-column interface, which was the case for Specimen 1. A similar cracking pattern was observed in an existing building with eccentric connections that was damaged in the 1995 Kobe Earthquake (Fig. 6), which shows that the testing procedure effectively simulates the earthquake loading. For this specimen, first spandrel beam flexural cracks and joint diagonal shear cracks formed at approximately 0.5% story drift. The damage correlates well with the maximum measured joint shear deformation of approximately 2.5%. For loading in the normal beam direction, flexural cracking of the normal beam and additional diagonal shear cracks in the joint were observed after 0.5% story drift. The cracking pattern indicates that the entire joint region of the rectangular column was working under applied loading.

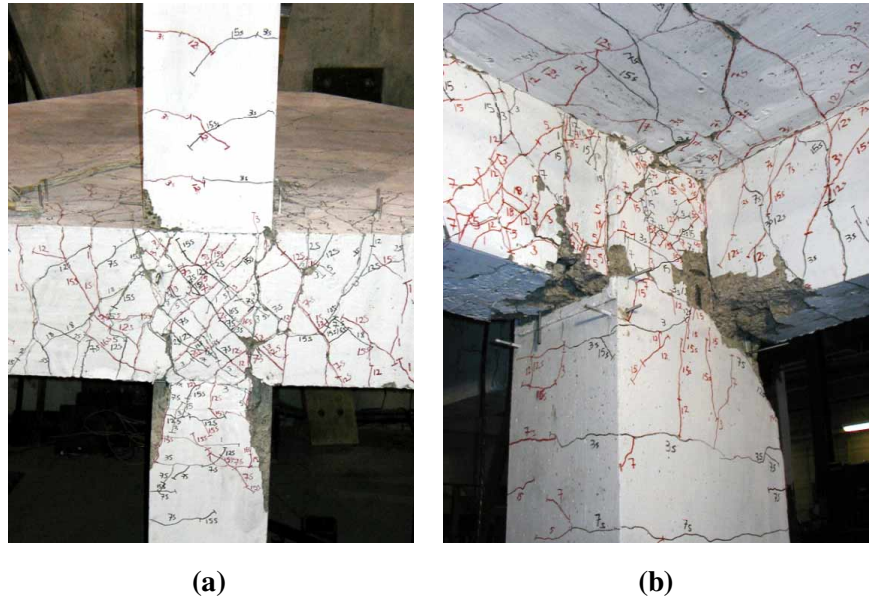


Figure 5: Cracking Pattern at the (a) Exterior and (b) Interior Faces of Specimen 2

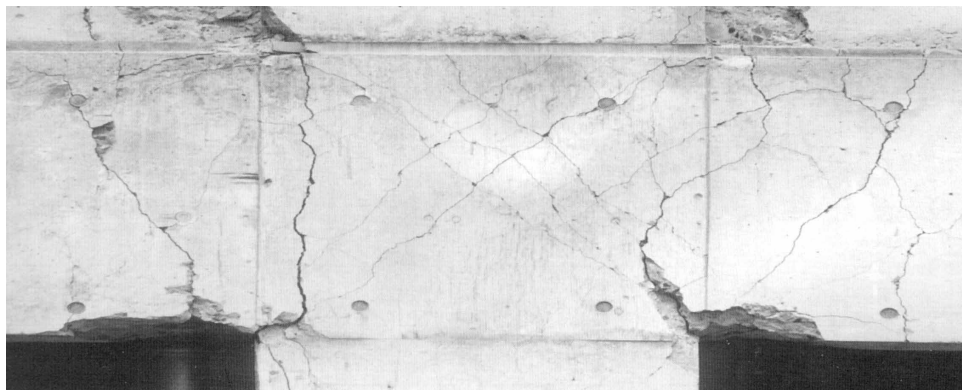


Figure 6: Cracking Pattern of a Building Damaged in 1995 Kobe Earthquake [5]

The overall cracking pattern observed in Specimen 3 (Fig. 7) was similar to that of Specimen 2. However, this specimen exhibited extensive spalling of concrete at the exterior face of the connection region due to the joint geometry. The wide normal beam could not confine the joint region as well as a regular normal beam; therefore, the damage was concentrated at the exterior face of the connection. For loading in the spandrel beam direction, flexural cracks opened at the face of the joint core region as in Specimen 2. First spandrel beam flexural cracks and joint diagonal shear cracks formed at approximately 0.5% story drift. For this specimen, the maximum measured joint shear deformation was 3.0%, which explains the extensive spalling of concrete. For loading in the normal beam direction, some spalling was observed in the normal beam due to a lack of confinement reinforcement for the wide beam bars that are anchored outside the column. In this direction, flexural cracking of the normal beam and additional diagonal shear cracks in the joint were observed at 1.0% story drift.



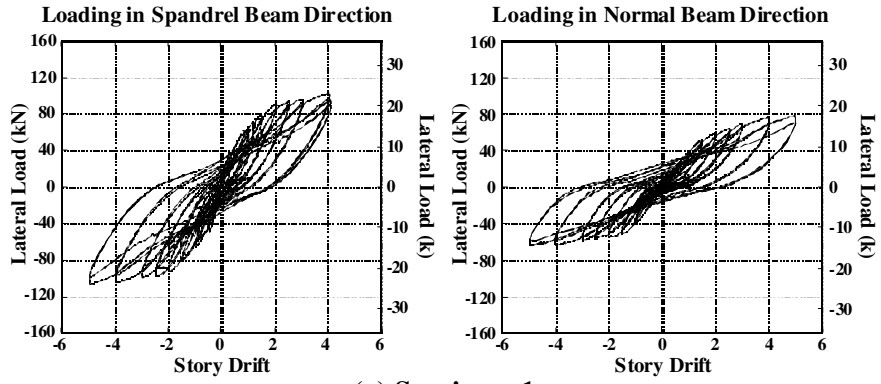
Figure 7: Cracking Pattern at the (a) Exterior and (b) Interior Faces of Specimen 3

Lateral Load versus Story Drift Response

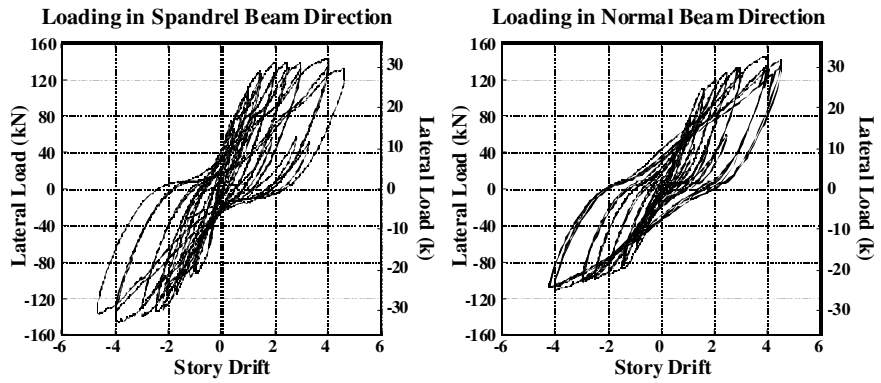
Previous test results [3, 4] showed that the eccentricity of the spandrel beam leads to early deterioration of the joint shear strength and excessive pinching of the load versus displacement hysteresis curves. However, as shown in Fig. 8a, Specimen 1 maintained its strength until the end of the test without any major pinching of the hysteresis curves for loading in both directions. When the behavior of Specimen 1 for loading in the spandrel beam direction was compared to a specimen tested by Raffaele and Wight [3], which had similar dimensions and reinforcement, a lower eccentricity level of 51 mm. (2 in.), but no floor slab and normal beam (Fig. 9), it is clear that including the floor system significantly improves the overall performance of eccentric connections and delays the deterioration of joint shear stiffness and strength. The maximum joint shear deformation observed in their two-dimensional specimen was 2%, which is twice the distortion observed in Specimen 1 of this experimental program. After 3% story drift in Specimen 1, when beam flexural deformations dominated the specimen response rather than diagonal cracking in the joint region, hysteresis curves became wider for loading in both directions, which shows the excellent energy dissipation capacity of this specimen.

There is slight pinching in the hysteresis curve of Specimen 2 for loading in the spandrel beam direction (Fig. 8b), and the specimen lost a small percentage of its strength after 4% story drift mainly due to the higher eccentricity level. However, the pinching is still not as severe as in Fig. 9, although the eccentricity is significantly higher. For loading in the normal beam direction, pinching was not observed because very few additional diagonal shear cracks formed in the joint.

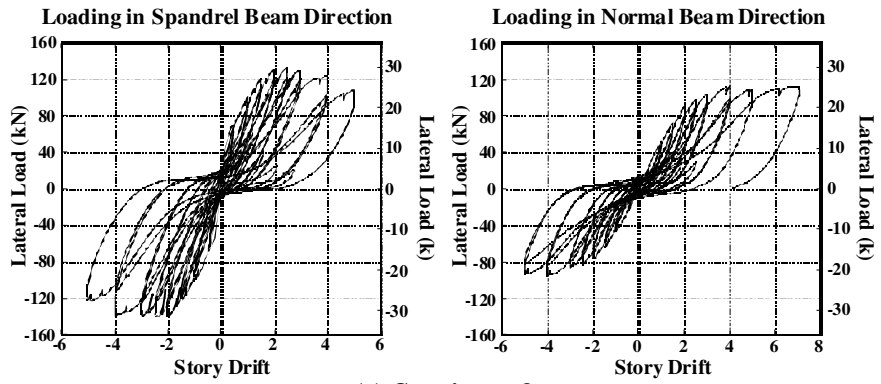
For loading in the spandrel beam direction, the lateral load versus story drift response of Specimen 3 (Fig. 8c) had more pinching than that of Specimen 2, due to the lack of confinement in the connection region resulting from the use of a wide normal beam. The total depth of the normal beam was less than three-quarters of the total depth of the spandrel beam, which is the minimum limit in the code [2]. The strength loss, which started after 3% story drift, was also higher in this specimen. Some pinching is observed for this specimen for loading in the normal beam direction due to the loss of anchorage for the wide beam longitudinal bars. The specimen was loaded to 7% story drift in the normal beam direction to observe the failure mode; however, it maintained its strength until the end of the test.



(a) Specimen 1



(b) Specimen 2



(c) Specimen 3

Figure 8: Lateral Load versus Story Drift Response of Test Specimens

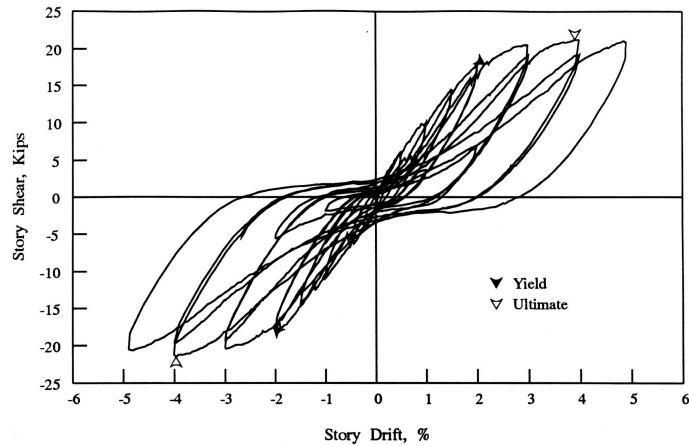


Figure 9: Pinched Hysteresis Curve of an Eccentric Beam-Column Connection in a Prior Test [3]

Moment versus Beam Plastic Hinge Rotation Response

The potentiometer layout on each face of the connection shown in Fig. 10 enabled the measurement of the beam plastic rotation and the concentrated rotation at the end of the beam. The beam plastic rotation is the rotation over the plastic hinging region caused by the flexural deformation of the beam. The end rotation is the concentrated rotation at the face of the joint due to the flexural cracks formed at the beam-to-column interface, joint shear deformation, and slip of beam reinforcement. The potentiometer that is touching the column face measures the total beam rotation, which is the sum of the beam plastic rotation and the end rotation. The potentiometer that is connected to a rod, which is placed adjacent to the column face, measures only the beam plastic rotation.

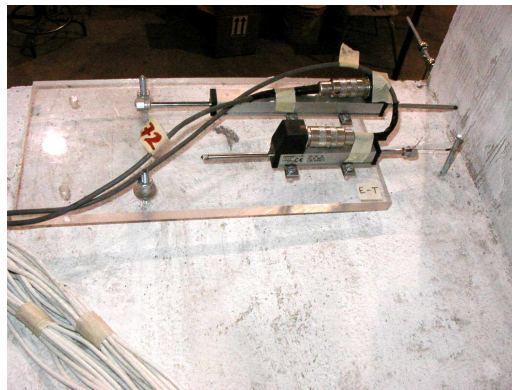
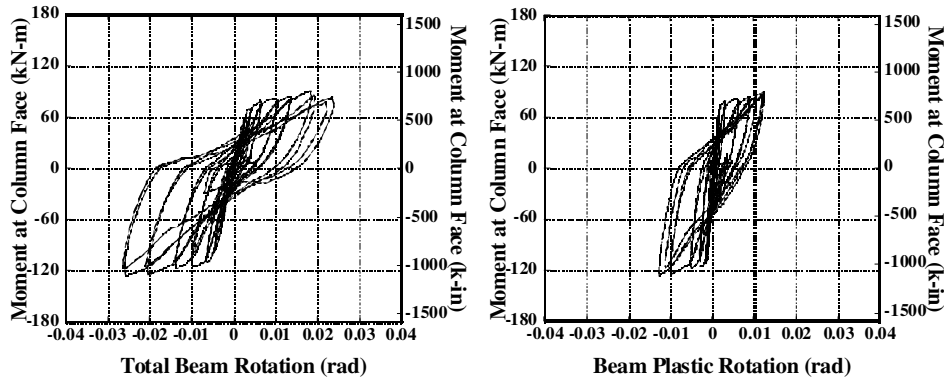


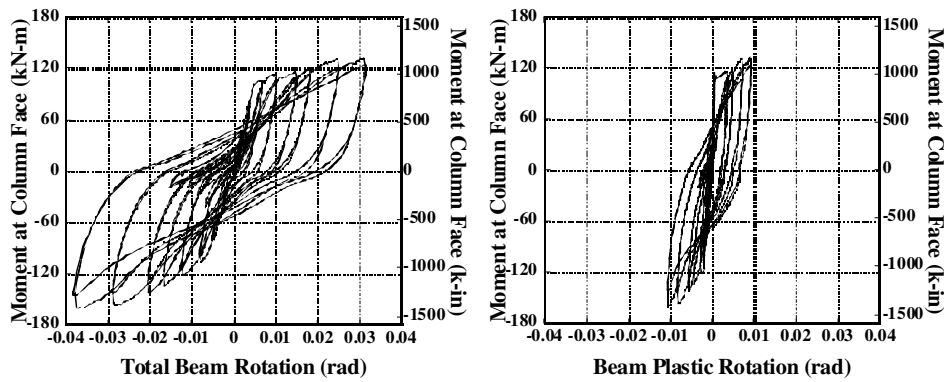
Figure 10: Potentiometer Layout to Measure Beam Rotations

The moment versus rotation diagrams for Specimen 1 are given in Fig. 11, as an example. The large beam rotations and the wide curves shown in these graphs points out that beam rotations contributed significantly to energy dissipation, especially at high drift levels. The data obtained from the potentiometers demonstrated that for loading in the spandrel beam direction, the contribution of the beam plastic rotation to the total beam rotation was lower than that for loading in the normal beam direction. The spandrel beam reinforcement yielded in all the tests and the nominal moment capacity of the spandrel beams was reached. Although, the yielding of some normal beam flange bars were at higher drift levels, the measured moment capacity of normal beams were very close to the design values at the end of each

test, except for Specimen 3, which had a wide beam as the normal beam. For loading in the normal beam direction, some of the strain gages that are placed on the flange bars did not reach the yield strain in all the tests. Detailed information on the spread of yielding is given elsewhere by the authors [7]. The reason for not reaching the yield strain is believed to be prior loading in the spandrel beam direction, which softened the joint and lowered the bond strength of the normal beam bars. This also increased the contribution of the end rotation to the total beam rotation in the normal beam direction.



(a) Loading in the Spandrel Beam Direction



(b) Loading in the Normal Beam Direction

Figure 11: Moment versus Beam Rotation Curves for Specimen 1

Energy Dissipation

The energy dissipated in each cycle was computed as the area enclosed by the hysteresis loops in the lateral load versus story drift curves. Then, these values were normalized by the energy dissipated during the first cycle to 1% story drift to account for strength differences of the specimens.

Fig. 12 shows the normalized energy dissipation capacity versus story drift response for Specimen 1, as an example. In this figure, the thick lines represent loading in the normal beam direction, while the thin lines are for loading in the spandrel beam direction. The solid lines represent the first cycles and the dashed lines are for the repeat cycles of each drift level. As can be observed in Fig. 12, the specimen dissipated more energy in the normal beam direction because the concentric beam forms a better mechanism than the eccentric one for dissipating energy. For the repeat cycles, the specimen lost 10 to 30 percent of its energy dissipation capacity from the first cycles.

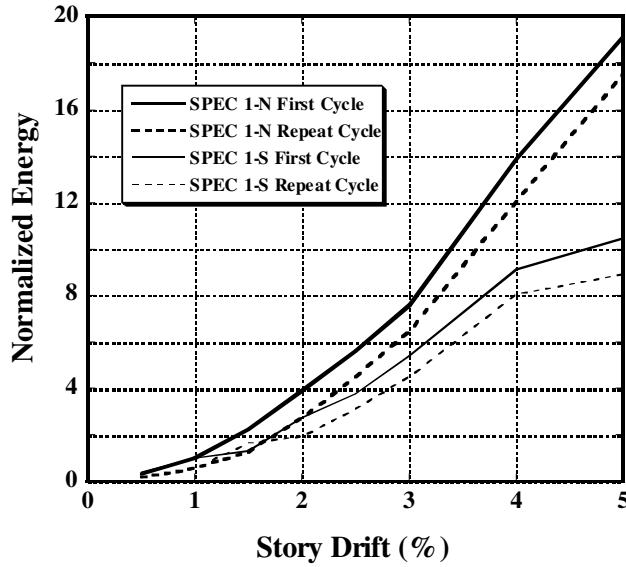


Figure 12: Normalized Energy Dissipation Capacity per Cycle for Specimen 1

The energy dissipation capacities of all three specimens for each new cycle to a specified drift level are compared in Fig. 13 for loading in the spandrel beam direction. Specimen 1, the specimen with the lower eccentricity, had the highest energy dissipation capacity. This is also confirmed with the wide hysteresis curves in lateral load versus story drift response of this specimen, which did not show any pinching (Fig. 8a). Specimen 2 experienced some pinching due to higher eccentricity, and thus had a lower energy dissipation capacity. Specimen 3, which had a lack of confinement in the joint region due to the use of a wide normal beam, had the lowest energy dissipation capacity. For Specimen 1, the dissipated energy per cycle increased with each new cycle, while for the last two specimens the energy dissipation increased up to 4.0% story drift level, then remained constant until the end of the test.

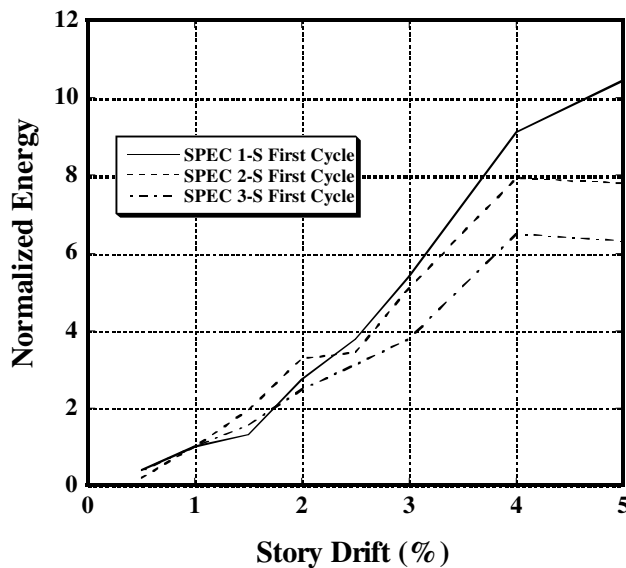


Figure 13: Comparison of the Normalized Energy Dissipation Capacity per Cycle

Stiffness Deterioration

The rate of stiffness deterioration is a measure of seismic performance of the connections. The stiffness of the specimens was computed as a peak-to-peak secant stiffness by using the maximum displacement and corresponding lateral load at each cycle. Then, the average values for stiffness in positive and negative loading directions were computed and they were normalized with respect to the average peak-to-peak stiffness of the first cycle to 1% story drift to account for different specimen parameters. Fig. 14 shows the normalized average stiffness versus story drift response of the specimens for loading in the spandrel beam direction. From this figure, it can be observed that the rate of stiffness deterioration was approximately the same for all specimens and at the end of the tests they had lost 75 to 85 percent of their initial stiffness. Specimen 1, which had the lower eccentricity and minor damage, lost 75 percent of its initial stiffness. Specimen 2, with a higher eccentricity, and Specimen 3, with a wide beam, lost higher percentages of their initial stiffness. For loading in the normal beam direction, the general trend was the same, but the specimens lost only 60 to 70 percent of their initial stiffness because concentric beams were used instead of eccentric ones.

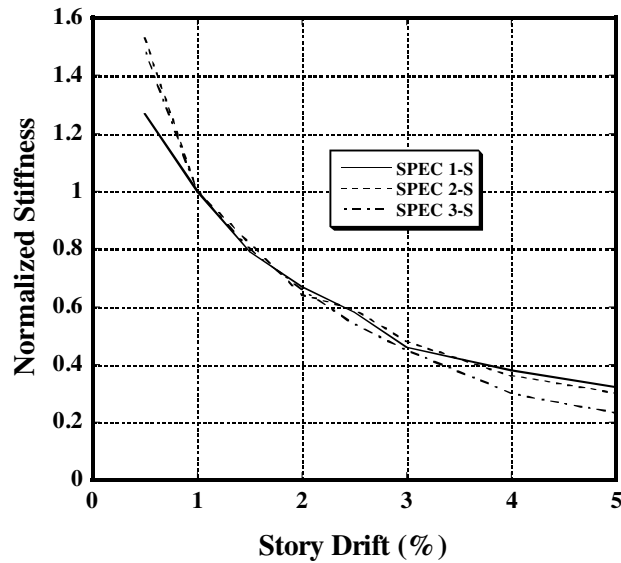


Figure 14: Normalized Average Peak-to-Peak Stiffness versus Story Drift Response of Specimens

CONCLUSIONS

The effect of eccentricity on the seismic behavior of exterior beam-to-column connections was investigated in this experimental program. Three approximately 3/4-scale exterior reinforced concrete beam-column-slab connections were tested under reversed cyclic loading. Two tests were performed on each specimen, first the lateral load was applied in the spandrel beam direction, then the specimen was rotated 90 degrees and the load was applied in the normal beam direction.

The major parameters for this investigation are the eccentricity of the spandrel beam with respect to the centroidal axis of the column, column section aspect ratio, and normal beam width. Specimen 1 was a control specimen designed according to the ACI code requirements [1, 2] with a square column, regular sized beams, and lower eccentricity. Specimen 2 had a higher eccentricity and a rectangular column with regular sized beams. In Specimen 3, a wide normal beam was used with a rectangular column and the level of joint stress was increased.

Experimental results on these eccentric beam-column-slab specimens demonstrated that including the floor system with the slab, spandrel, and normal beams adds considerable torsional stiffness to the subassembly and delays the deterioration of the joint shear stiffness and strength. In spite of the high eccentricity levels, nominal moment capacity of the spandrel beams was reached in all the tests. The measured moment capacity of normal beams were very close to the design values for the first two tests, although the capacity was reached at higher drift levels due to the reduced stiffness of the subassembly resulting from the prior loading in the spandrel beam direction. The softening of the joint region due to prior loading did not significantly affect the joint shear strength. In highly eccentric specimens, diagonal shear cracks were observed primarily within the core region of the joint. Therefore, the column core dimension rather than the full column width should be taken as the development length for the spandrel beam bars in eccentric beam-to-column connections. For connections in wide-beam structures, additional confinement reinforcement is required to prevent concrete crushing and loss of anchorage for the wide beam bars that are not placed within the column. For joints with rectangular columns, it was observed that as long as the column section aspect ratio (width vs. depth) was kept less than or equal to 1.5, the entire section of the column worked to resist the joint shear stresses applied by the floor system.

ACKNOWLEDGEMENT

This research study was sponsored by the National Science Foundation under the Grant No. CMS 9812464. The conclusions contained in this paper are those of the authors and do not necessarily represent the view of the sponsor.

REFERENCES

1. ACI-ASCE Committee 352, "Recommendations for Design of Beam-Column Connections in Monolithic Reinforced Concrete Structures," ACI 352-R01, American Concrete Institute, Farmington Hills, Michigan, 2001.
2. ACI Committee 318, "Building Code Requirements for Structural Concrete," ACI 318-99, American Concrete Institute, Farmington Hills, Michigan, 1999.
3. Raffaele, G.S., and Wight, J.K., "Reinforced Concrete Eccentric Beam-Column Connections Subjected to Earthquake-Type Loading," ACI Structural Journal, Vol. 92, No. 1, pp. 45-55, 1995.
4. Lawrence, G.M., Beattie, J.H., and Jacks, D.H., "Cyclic Load Performance of an Eccentric Beam Column Joint," Central Laboratories Report 91-25126, Central Laboratories, Lower Hutt, New Zealand, 1991.
5. Arai-Gumi Technical Research Institute, "Special Issue Investigation Report on the 1995 Hyogen-Nambu Earthquake," Arai Technical Research Report, Hyogo, Japan, 1999.
6. Ohno, K., and Shibata, T., "On the Damage to the Hakodate College by the Tokachioki Earthquake, 1968," Proceedings of the U.S.-Japan Seminar on Earthquake Engineering with Emphasis on the Safety of School Buildings, pp. 129-144, 1970.
7. Burak, B., Wight, J. K., "Seismic Behavior of Eccentric Reinforced Concrete Beam-Column-Slab Connections under Sequential Loading in Two Principal Directions," Proceedings, ACI Fifth International Conference on Innovation in Design with Emphasis on Seismic, Wind and Environmental Loading; Quality Control and Innovation in Materials/Hot Weather Concreting, SP 209, Cancun, Mexico, pp. 863-880, 2002.